Mathematical Models for physical interactions of robots with their environment

Adam Stager and Herbert Tanner

Department of Mechanical Engineering, University of Delaware
{astager,btanner}@udel.edu

1 Introduction

Planning algorithms and navigation strategies have almost entirely aimed at avoiding collisions, with the obstacles and workspace boundaries serving to impose constraints on robot paths [1]. In the past, robots structural and internal components were expensive, fragile, and in general not considered dispensable, which clearly motivated the urge for collision avoidance. Today, however, new methods for manufacturing and the development of affordable, smaller scale electronics have enabled the development of a different class of robots that can either withstand collisions, or be considered dispensable when they do not always survive them. There has even been evidence that robotic missions can benefit from contact with the environment [2, 3]. Yet efforts to understand, implement, and exploit such behaviors are still at their infancy.

Boundary following is one exception, having its roots in early bug algorithms where the presence of obstacles actually allows provable convergence [4]. In fact, insects commonly collide with their boundaries continuing with no ill-effect [5]. Several aerial robots have been developed demonstrating similar behavior, with intentional mechanisms adding robustness to collisions [6, 7]. Early work demonstrates the potential for physical robot-environment interaction to contribute in new strategies for motion planning [8].

Compared to aerial robots, ground mobile robots offer more room for the designer to make them robust to collisions, add shielding, and even employ mechanisms to exploit boundary interactions. Small-scale platforms in particular, have been shown to benefit by colliding with their boundary; traveling on new, sometimes improved paths after a collision [3], or offering a foothold to improve mobility after a collision [9].

Despite progress toward developing robust, collision resistant platforms, mathematical models that capture impact behavior, and planners that intensionally incorporate these behaviors are currently under-developed. One model that has been used to capture reflections in terms of a coefficient of restitution [10], provides a simplified proof of concept, but it does not go as far as capturing the uncertainty that is inherent in robot-boundary interaction. A *stochastic* model that could capture the mechanics of collision, recovery, as well as failure, could be particularly useful in exploiting such phenomena in low-friction or high speed scenarios [11].

This paper identifies such a model, based on existing mathematical models for partially reflected diffusions [12]. We construct a ground mobile robot

called Omnipuck as an experimental testbed for validating the hypothesis that the mathematics of partially reflected diffusions fit well in the context of robot-environment collisions. Omnipuck is designed to benefit from impact events by storing/releasing potential energy during collisions. The preliminary results reported in this paper have utilized the Omnipuck to match probability distribution parameters and thus compare analytical results to experimental reflection data. The results suggest that the partially reflected diffusion model shows promise in describing robot-environment physical interaction phenomena, as well as predicting not only the aftermath of collisions (excluding the possibility of failure, at this moment) but also the evolution of the system during the process.

2 Technical Approach

Post collision behavior is studied as a partially reflected diffusion [12], capturing the position of the robot after surviving a collision in the form of a distribution. An absorption parameter controls the rate at which sample paths reaching the bandwidth are not reflected back —this percentage models the rate at which collisions lead to failure. The stochastic model seems appropriate to capture not only the possible variability in the motion of the robot during the collision phase, and the uncertainty regarding both the contact point, as well as the location the robot will find itself after bouncing off.

Partially reflected diffusions [12] are characterized by a drift term $a(x,t)$, and a diffusion term $\sigma(x,t) > 0$. In practice, these terms —especially the latter— are experimentally estimated. In this paper, we assume decoupled motion along each direction, assumption which allows the analysis to proceed with a single-dimensional model for the motion along each direction.

If x expresses the state (read: position) of a particle along a positive semiaxis (with zero marking the workspace's boundary), then the stochastic motion of the particle may be modeled as

$$\mathrm{d}x = a(x,t)\,\mathrm{d}t + \sqrt{2\sigma(x,t)}\,\mathrm{d}w \tag{1}$$

The solution of (1) with partially absorbing boundaries has been defined [12] to be the limit of the solutions of a Markov jump process $x_{\Delta t}$, which for $s \leq t \leq s+T < \infty$ and $\Delta t = \frac{T}{N}$ for $N \in \mathbb{N}$, is generated by the Euler scheme

$$\begin{aligned} x_{\Delta t}(s) &= x \\ x_{\Delta t}(t+\Delta t) &= x_{\Delta t(t)} + a\big(x_{\Delta t}(t),t\big)\,\Delta t + \sqrt{2\sigma\big(x_{\Delta t}(t),t\big)}\,\Delta w(t,\Delta t) \end{aligned} \tag{2}$$

where the random variables Δw are normally distributed with zero mean and variance Δt. In the Euler scheme of (2), the absorption at the boundary is modeled through the boundary conditions. Let R denote the probability of reflection, i.e., the event that the robot bounces off undamaged, and define [12]

$$P \triangleq \lim_{\Delta t \to 0} \frac{1-R}{\sqrt{\Delta t}}$$

Then the boundary conditions for (2) are activated whenever it is detected that the next iterate of (2) has crossed the (zero) boundary, namely when

$$x_{\Delta t(t)} + a\big(x_{\Delta t}(t), t\big)\,\Delta t + \sqrt{2\sigma\big(x_{\Delta t}(t), t\big)}\,\Delta w(t, \Delta t) < 0$$

in which case it is reset to

$$x_{\Delta t}(t + \Delta \mathrm{t}) := \begin{cases} x_{\Delta t(t)} + a\big(x_{\Delta t}(t), t\big)\,\Delta t + \sqrt{2\sigma\big(x_{\Delta t}(t), t\big)}\,\Delta w(t, \Delta t) & \text{w.p } 1 - P\sqrt{\Delta t} \\ \text{process terminates} & \text{w.p. } P\sqrt{\Delta t} \end{cases} \tag{3}$$

When the process terminates in (3) it is understood as a catastrophic failure of the robot after the collision.

The Fokker-Planck equation (FPE) associated with (1) is [12]

$$\frac{\partial p(y,t|x,s)}{\partial t} = -\frac{\partial\, a(y,t)\, p(y,t|x,s)}{\partial y} + \frac{\partial^2\, \sigma(y,t)\, p(y,t|x,s)}{\partial y^2} \tag{4}$$

with initial condition $p(y,t|x,s) \to \delta(y-x)$ as $t \downarrow s$, and radiation boundary condition

$$a(0,t)\, p(0,t|x,s) - \frac{\partial\, \sigma(0,t)\, p(0,t|x,s)}{\partial y} = -\kappa\, p(0,t|x,s)$$

with $\kappa = \frac{P\sqrt{\sigma(0,t)}}{\sqrt{\pi}}$ denoting the reactive coefficient related to the probability of absorption at the boundary $y = 0$ [12].

In one dimension, and for constant a and σ, the FPE (4) has an explicit solution with initial condition $x(0) = x_0$ [12]

$$\begin{aligned} p(x,t|x_0) = {} & \\ & \frac{a}{\sqrt{4\pi\sigma t}}\left[\exp\left\{-\frac{(x-x_0-at)^2}{4\sigma t}\right\} + \exp\left\{-\frac{ax_0}{\sigma} - \frac{(x-x_0-at)^2}{4\sigma t}\right\}\right] \\ & - \frac{2\kappa + a}{2\sigma}\exp\left\{\frac{ax + \kappa\big[x + x_0 + (\kappa + a)t\big]}{\sigma}\right\}\operatorname{erfc}\left[\frac{x + x_0 + (2\kappa + a)t}{\sqrt{4\sigma t}}\right] \end{aligned} \tag{5}$$

The goal now is to express the distribution of the location of the robot *after* impact, and as soon as it is capable of reassuming control of its motion, by a probability distribution function of the form (5), with time t counting from the time of impact (Fig. 1).

In order to validate the hypothesis that (5) can capture the outcome of workspace boundary collisions, at least in a single-dimension, we constructed a collision -tolerant, omni-directional ground mobile robot (Fig. 2). Its omni-directional wheels allow it to independently generate motion along directions

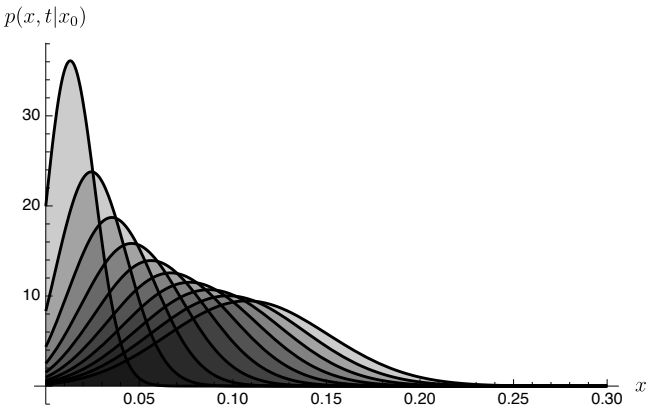

Fig. 1. How the density given in (5) changes over time. As time t increases, the peak of $p(x,t|x_0)$ shifts to the right of the boundary $x = 0$.

on the Cartesian plane A specially designed ring surround the robot including embedded springs that allow impact energy to be stored and redirected. The Omnipuck was designed by a combination of 3D printing and off-the-shelf components. This afforded flexibility for iteration of the design and reduced the time and cost of assembling the platform. The omni-wheels can be used in multiple configurations; in this particular case, three wheels were chosen because they maintain consistent ground contact and require only three motors controlling the origin of a body centered robot frame in $\mathbb{R}^2$.

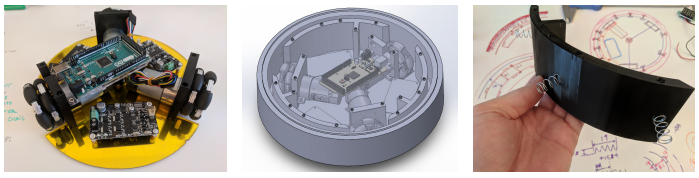

(a) (b) (c)

Fig. 2. The Omnipuck robot constructed to study workspace boundary reflections. (a) an Atmega 328 micro-controller sits at the core of the Omnipuck and controls motors through PWM to three independent motor controllers; (b) a reflection ring provides robustness to collision while storing/redirecting impact energy; (c) nine equally spaced springs encompass the robots perimeter.

3 Results

The parameters of the reflection model (5) are estimated experimentally, based on a body of trajectory data collected from 500 head-on collisions with the Omnipuck. Each one of these experiments proceeded as follows. The robot was positioned automatically to the same initial position, at a distance of $x_0 = 1.866$

m relative to the reflection boundary, and then commanded to travel in a straight line perpendicular into a synthetic wall boundary at a velocity of 2 m/s. Data collection for the experiment ceases when the collision is detected by the on-board accelerometer. For this body of data, a final time of $t = 2.366$ seconds, and setting $\kappa = 0$ (pure reflection), the parameters of (5) were estimated at $a = 0.01943$ and $\sigma = 2.9145 \times 10^{-5}$.

A histogram of the final positions recorded is shown in Fig. 3(a), where one can also see an empirical probability distribution function is fitted over these data. Next to this figure, in Fig. 3(b) one can see how this empirical density function compares to the theoretical model (5) when parameterized with the estimated values of a and σ given above.

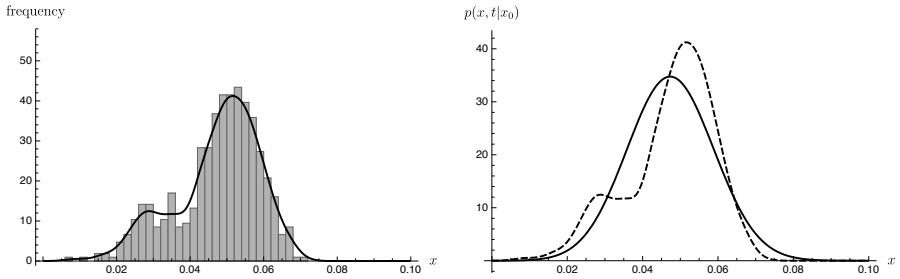

Fig. 3. Matching data to model. (a) a histogram of the positions recorded at (total) time $t = 2.366$, and an empirical density function that is constructed based on the histogram; (b) comparison of the empirical density (dashed) with the model (5).

We anticipate that if a larger sample size becomes available, the bi-modal aspect of the empirical distribution of Fig. 3(a) will subside, allowing even better matching to the theoretical model.

4 Scheduled Experiments

The results obtained herein will be extended in three ways. First, we will test the efficacy of the partially reflected diffusion model for capturing reflection behaviors at different wall angles and velocities. We will identify nominal model parameters that best capture experimental data and support the hypothesis that reflection behaviors can be well captured by a partially reflected diffusion model.

Next, we will collect N=250 sample paths for $30, 45, 60$ degree collision angles and provide these results as a set of motion primitives for extension into planning and navigation strategies. Finally, we will quantitatively compare "there-and-back" experiments for free space and reflection scenarios in order to validate the proposed benefits.

5 Main Experimental Insights

The preliminary analysis conducted suggests that the effect of physical robot-environment interactions on the robot position can be captured in the form of analytically defined probability distributions with parameters capable of capturing not only the location of the robot after impact, but also the possibility for terminal, catastrophic collisions. The theoretical model suggested shows promise in being able to describe this phenomenon probabilistically, and thus develop into a crucial component of motion planners that seek to exploit collisions between robust (or dispensable) robot designs and their surrounding environment, when the trade-offs between the risk of failure and the probability of improving mission objectives through collisions appear favorable.

References

1. S. M. LaValle, *Planning Algorithms*. Cambridge University Press, 2006.
2. A. Briod, P. Kornatowski, A. Klaptocz, A. Garnier, M. Pagnamenta, J.-C. Zufferey, and D. Floreano, "Contact-based navigation for an autonomous flying robot," *IEEE/RSJ International Conference on Intelligent Robots and Systems*, pp. 3987–3992, 2013.
3. K. Karydis, D. Zarrouk, I. Poulakakis, R. S. Fearing, and H. G. Tanner, "Planning with the STAR(s)," in *Proceedings of the IEEE/RSJ International Conference on Intelligent Robots and Systems*, 2014, pp. 3033–3038.
4. V. J. Lumelski and A. A. Stepanov, "Dynamic Path Planning for a Mobile Automaton with Limited Information on the Environment," *Ieee Transactions on Automatic Control*, vol. 31, no. 11, pp. 1058–1063, 1986.
5. A. Briod, "Observation of Insect Collisions," Ph.D. dissertation, Harvard University, 2008.
6. A. Briod, P. Kornatowski, A. Klaptocz, A. Garnier, M. Pagnamenta, J. C. Zufferey, and D. Floreano, "Contact-based navigation for an autonomous flying robot," *IEEE International Conference on Intelligent Robots and Systems*, pp. 3987–3992, 2013.
7. Y. Mulgaonkar, G. Cross, and V. Kumar, "Design of small, safe and robust quadrotor swarms," *Proceedings - IEEE International Conference on Robotics and Automation*, vol. 2015-June, no. June, pp. 2208–2215, 2015.
8. Y. Mulgaonkar, A. Makineni, L. Guerrero-Bonilla, and V. Kumar, "Robust Aerial Robot Swarms Without Collision Avoidance," *IEEE Robotics and Automation Letters*, vol. 3, no. 1, pp. 596–603, 2018.
9. D. W. Haldane, M. M. Plecnik, J. K. Yim, and R. S. Fearing, "Robotic vertical jumping agility via series-elastic power modulation," *Science Robotics*, vol. 1, no. 1, p. eaag2048, 2016.
10. R. L. Garwin, "Kinematics of an Ultraelastic Rough Ball," *American Journal of Physics*, vol. 37, no. 1, p. 88, 1969.
11. S. Karaman and E. Frazzoli, "High-speed motion with limited sensing range in a poisson forest," *Proceedings of the IEEE Conference on Decision and Control*, pp. 3735–3740, 2012.
12. A. Singer, Z. Schuss, A. Osipov, and D. Holcman, "Partially Reflected Diffusion," *SIAM Journal on Applied Mathematics*, vol. 68, no. 3, pp. 844–868, 2008.